Robust regenerator allocation in nonlinear flexible-grid optical networks with time-varying data rates

Citation for the original published paper (version of record):
Yan, L., Xu, Y., Brandt-Pearce, M. et al (2018). Robust regenerator allocation in nonlinear flexible-grid optical networks with time-varying
data rates. Journal of Optical Communications and Networking, 10(11): 823-831.
http://dx.doi.org/10.1364/JOCN.10.000823

Robust Regenerator Allocation in Nonlinear Flexible-Grid Optical Networks With Time-Varying Data Rates

Li Yan, Yuxin Xu, Maïté Brandt-Pearce, Nishan Dharmaweera, and Erik Agrell

***Abstract*—Predeployment of regenerators in a selected subset of network nodes allows service providers to achieve rapid provisioning of traffic demands, high utilization, and reduced network operational costs, while still guaranteeing lightpaths quality of transmission. Enabled by bandwidth-variable transceivers in flexible-grid optical networks, optical channel bandwidths are no longer fixed but constantly changing according to real-time communication requirements. Consequently, the data-rate-variable traffic together with other new network features introduced by flexible-grid networks will render the regenerator allocation very difficult due to the complicated network states. In this paper, we investigate how to allocate regenerators robustly in flexible-grid optical networks to combat physical layer impairments when data rates of traffic demands are random variables. The Gaussian noise model and a modified statistical network assessment process framework are used to characterize probabilistic distributions of physical-layer impairments for each demand, based on which a heuristic algorithm is proposed to select a set of regenerator sites with the minimum blocking probability. Our method achieves the same blocking probabilities with on average 10% less regenerator sites compared with the greedy constrained-routing regenerator allocation method, and obtains two orders of magnitude lower blocking probabilities than the routing and reach method with the same numbers of regenerator sites.**

***Index Terms*—Network optimization; Regenerator placement; Physical-layer impairments; Variable traffic.**

I. Introduction

The rapid rise in the use of the mobile Internet, video streaming, and cloud computing services has led to increasing data volumes and diversified traffic requests, which put severe pressure on backbone optical networks. Flexible-grid optical networks have been proposed to relax the rigid spectrum grid requirement of wavelength-division multiplexing (WDM) networks and offer much higher efficiency by adaptively assigning spectrum to traffic demands [1].

Moreover, new network and transmission techniques are also introduced to further improve the network capacity. Enabled by bandwidth-variable wavelength cross-connects (BV-WXCs) and bandwidth-variable transceivers (BV-Ts), network operators can dynamically change the bandwidths of optical channels according to real-time communication requirements and, thus, achieve cost-effective and highly available connectivity services [2]. Additionally, the advent of higher-order modulation formats and variable coding-rate schemes [3]–[5] will allow finer granularity of spectrum efficiency in transmission systems. Consequently, the state of the network[1] becomes extremely complicated and physical-layer impairments (PLIs) will be the dominant limitation for satisfactory lightpath quality of transmission (QoT) and optical reach.

In flexible-grid optical networks, to achieve long-haul transmission between nodes, one or more optoelectronic regenerators may have to be used to restore optical signals. However, each regenerator adds a cost comparable to a pair of endpoint transceivers [6] and, thus, requires system operators to predeploy them as efficiently as possible. By deploying regenerators at a subset of the network nodes, referred to as regenerator sites (RSs), we can achieve better sharing of spare regenerators for randomly variable demands and improved operational efficiency by requiring fewer truck rolls [7], which require to dispatch technicians in a truck to install or maintain the network equipment.

The problem of allocating a minimum set of RSs is defined as the regenerator location problem (RLP) [6]. Previous studies have investigated the RLP in single-line rate or waveband-switched WDM networks from cost and energy consumption perspectives [6]–[10]. Efficient heuristic algorithms have also been proposed to find RSs in mixed-line rate WDM networks [11], [12]. However, this research either assumes detailed PLIs as known system parameters [8], [9], or rely on the transmission reach (TR) model [6], [7], [11]–[13], which represents the impairments as reachability in the worst case with fiber links fully loaded.

Another issue with the existing studies is that their solutions are all based on static traffic models where both the set of traffic demands and their data rates are fixed. Although the set of traffic demands remains relatively stable in the current backbone optical networks [14]–[16], the data rates of traffic demands are usually random variables varying according to real-time requirements. Provided that the flexible-grid enabling BV-WXC and BV-T technologies [2] are utilized, the corresponding optical channel bandwidths in the network are random variables as well. Consequently, RLP solutions based on static traffic predictions become inaccurate and inefficient in the variable-traffic operation scenario.

In this paper, we consider the RLP in nonlinear flexible-grid networks, where the data rates of traffic demands are random

Manuscript received XXX. xx, 2017; revised XXX. xx, 2017; accepted XXX. xx, 2017; published XXX. xx, 2017.

L. Yan, E. Agrell, and N. Dharmaweera are with Chalmers University of Technology, Gothenburg SE-41296, Sweden (e-mail: lyaa@chalmers.se).

Y. Xu and M. Brandt-Pearce are with University of Virginia, Charlottesville 22904, Virginia, USA

[1]In this paper, the state of flexible-grid optical networks refers to the occupancy of all the resources in the network and determines the network utilization and physical-layer impairments.

Table I: PARAMETERS IN THE PROBLEM STATEMENT

Symbol	Meaning
V	the set of nodes
E	the set of links
b_{sub}	the subcarrier bandwidth (in GHz) in the network
M	the name of the modulation format used in the network
c	the spectral efficiency of M
G	the PSD (in W·THz^{-1}) used for all the traffic demands
SNR_{th}	the SNR threshold of M to achieve an acceptable QoT
T	the set of traffic demands
R_t	a random variable representing the data rate (in Gbps) of demand $t \in T$
$p_{R_t}(r_t)$	the PDF of the data rate for demand $t \in T$
Δb_t	the optical channel bandwidth (in GHz) of demand $t \in T$
F_{max}	the maximum number of RSs in the network
$S(F_{\text{max}})$	the set of output RSs whose total number is constrained by F_{max}

variables. The PLI are characterized using the Gaussian noise (GN) model [17]–[19] and a modified statistical network assessment process (SNAP) framework [20], based on which a robust RLP algorithm is implemented. The proposed method is compared with two previous algorithms [6], [10] that are based on the TR model and static traffic prediction. The impact of data-rate-variable traffic on RS allocation is also studied.

The remainder of this paper is organized as follows. In Section II, the RLP in nonlinear flexible-grid networks with variable traffic is described. Our proposed algorithm is presented in Section III. Section IV presents and discusses numerical results. We conclude the paper in Section V.

II. PROBLEM STATEMENT

In this paper, we consider an optical network represented by an undirected graph with sets of nodes V and links E, where each link $l \in E$ is a bidirectional dispersion-uncompensated fiber link between nodes i and j for $i, j \in V$. The spectrum on each fiber is sliced into subcarriers with a bandwidth of b_{sub} (in GHz). All traffic demands are assumed to use a uniform power spectral density (PSD) G (in W·THz^{-1}) and the same modulation format M with a spectral efficiency c and signal-to-noise ratio (SNR) threshold SNR_{th} that guarantees an acceptable QoT. A guardband with bandwidth of b_{sub} is assigned to each traffic demand.

A static and known set of traffic demands T is assumed in this study. Each element $t \in T$ is associated with its source s, destination d for $s \neq d$ and $s, d \in V$, and a time-varying random variable R_t representing its instantaneous data rate (in Gbps) including forward error correction (FEC) overhead. A probability density function (PDF) $p_{R_t}(r_t)$ is used to represent its distribution. By employing Nyquist spectral shaping [21], the demand t with data rate r_t has a bandwidth of $\Delta b_t = b_{\text{sub}} \cdot \lceil r_t/(b_{\text{sub}} \cdot c) \rceil$. The push-pull technique [22] and dynamic lightpath adaptation algorithm [23], [24] are used to adjust bandwidth and shift carrier frequencies of optical channels without disruption. The spectrum ordering of demands is also assumed random, because the traffic loading process is usually unknown to the RLP, which is solved in the early stages of the network planning, and the spectrum assignment will probably change after restorations from network failures. In response to the time-varying data rates and spectrum ordering, the transceivers and switches in the network are reconfigured periodically after fixed time intervals.

As functions of the data rates and spectrum ordering, the SNRs of traffic demands are also varying in time. A blocking happens when the temporary SNR of a demand is lower than SNR_{th}. To achieve efficient network operation, we assume that the temporarily blocked demands are still present in the network instead of being rejected and reconnected frequently. The noise blocking probability (BP) in this study is thus defined as the overall blocking probability averaged over time.

Based on the above-mentioned description, our RLP takes as input parameters: the network topology (V, E), subcarrier bandwidth b_{sub}, available modulation format M with spectral efficiency c, uniform PSD G, maximum number of RSs F_{max}, and set of data-rate-variable demands T with known $p_{R_t}(r_t)$ for $t \in T$. The output is a set of RSs, denoted as $S(F_{\text{max}})$, that minimizes the BP. The input and output parameters of the proposed regenerator allocation algorithm are listed in Table I.

III. REGENERATOR SITE ALLOCATION ALGORITHM

The modified SNAP framework that simulates PLI noise distributions for each demand–link pair is discussed in Section III-A. Then we present the RS allocation algorithm in Section III-B. The parameters used in this section are listed in Table II.

A. Modified Statistical Network Assessment Process

The GN model [17]–[19] is an analytical model to account for the nonlinear interference (NLI) caused by the Kerr effect. It takes the allocation of routes, spectral orderings, and bandwidths of all the traffic demands as input and calculates the PLI noise for each demand–link pair $(t, l), \forall t \in T, l \in P_t$, where $P_t \subset E$ denotes the ordered set of links on the route of t. Based on the GN model, the PLI noise suffered by a demand is the sum of its NLI noise and the additive spontaneous emission (ASE) noise introduced by optical amplifiers on its route. Therefore, under the condition that the data rates and spectrum orderings of all the demands in the network are random variables, the PLI noises for all the demand–link pairs are random variables as well.

The probabilistic distribution of PLI noise suffered by each demand–link pair is critical in quantifying the BP and achieving a robust regenerator placement. In this study, a modified version of the SNAP [20] is used to draw samples from the state space of the network and statistically characterize the PLI noise distributions. The flowchart of the modified SNAP is shown in Fig. 1.

The modified SNAP used in this study takes as input the following information:

1) The traffic model including the set of traffic demands T and the probabilistic distribution $p_{R_t}(r_t)$ for $t \in T$.
2) The routing and spectrum assignment policy.
3) The network topology (V, E).
4) Transmission and physical-layer parameters for PLI evaluation, i.e., the modulation format of optical signals,

Table II: PARAMETERS IN THE PROPOSED ALGORITHM

Symbol	Meaning
P_t	the ordered set of links on the route of $t \in T$
Q_t	the ordered set of intermediate nodes on the route of $t \in T$
$\mathcal{L}(T)$	the ordered list of randomly shuffled demands in T
N_{MC}	the number of Monte Carlo repetitions
$N_{t,l}$	the random noise of the demand $t \in T$ on the link $l \in P_t$
$p_{N_{t,l}}(n)$	the PDF of $N_{t,l}$
f_i	a binary indicator that equals 1 if node $i \in V$ is an RS and 0 otherwise
$\mathbf{f}$	$\mathbf{f} = \{f_1, \ldots, f_{\lvert V\rvert}\}$ is a vector of f_i for $i \in V$
$H_t(\mathbf{f})$	the BP of the demand $t \in T$
$\texttt{Seg}(t, \mathbf{f})$	the set of transparent segments on the route of the demand $t \in T$ that is divided by the RS allocation $\mathbf{f}$
$\texttt{Seg}(t)$	the set of all possible transparent segments on the route of the demand $t \in T$
N_t^s	a random variable denoting the accumulated noise of the demand $t \in T$ at the end of the transparent segment $s \in \texttt{Seg}(t)$
$p_{N_t^s}(n)$	the PDF of N_t^s
H_t^s	the BP of the demand $t \in T$ on the transparent segment $s \in \texttt{Seg}(t)$
$\texttt{src}(x)$	the source of x, where x can be a demand, link, or a transparent segment
$\texttt{dst}(x)$	the destination of x, where x can be a demand, link, or a transparent segment
$\bar{V}_t$	$\bar{V}_t = \{\texttt{src}(t), \texttt{dst}(t)\} \cup Q_t$ for $t \in T$
w_s	the weight associated with the link $s \in \texttt{Seg}(t)$
$\bar{D}_t$	the auxiliary weighted complete graph $\bar{D}_t = (\bar{V}_t, \texttt{Seg}(t))$ with weight w_s for the link $s \in \texttt{Seg}(t)$
$\mathcal{S}_t$	the set of promising RS allocations for $t \in T$
$\mathcal{S}_{t,k}$	the set of promising RS allocations with exactly k transparent segments for $t \in T$
K	the maximum number of different solutions that will be collected in $\mathcal{S}_{t,k}$
u_s	a binary variable that equals 1 if the transparent segment $s \in \texttt{Seg}(t)$ has its sourse and destinations as RSs, the source, or the destination of $t \in T$ and 0 otherwise
u_s^κ	the value of u_s in the κ-th element of $\mathcal{S}_{t,k}$ for $\kappa \in \{1, \ldots, \lvert\mathcal{S}_{t,k}\rvert\}$
$\mathcal{U}_t$	$\mathcal{U}_t = \{1, \ldots, \lvert\mathcal{S}_t\rvert\}$, the set of indices for elements in $\mathcal{S}_t$
$\mathbf{f}^{t,\kappa}$	the κ-th element in $\mathcal{S}_t$ for $\kappa \in \mathcal{U}_t$
$y_{t,\kappa}$	the binary variable that equals 1 if the precalculated solution $\mathbf{f}^{t,\kappa} \in \mathcal{S}_t$ is chosen by the overall RS allocation and 0 otherwise, $\kappa \in \mathcal{U}_t$
z_i	the binary variable that equals 1 if the node $i \in V$ is chosen by the overall RS allocation and 0 otherwise
θ	a large enough real number

the PSD assignment policy, and the fiber and optical amplifier parameters, etc.

The modified SNAP outputs the PLI distributions for each demand–link pair by performing a Monte Carlo analysis. During each Monte Carlo run, a progressive load of the network is carried out to simulate one possible resource usage state of the network:

1) Shuffle the demands randomly and generate an ordered list of demands $\mathcal{L}(T)$.
2) Draw a random sample of the data rate from the PDF $p_{R_t}(r_t)$ for each $t \in T$.
3) Load demands with the order in $\mathcal{L}(T)$ and data rates generated at the step 2.
4) Calculate the PLI for each demand–link pair based on the GN model, the demand bandwidths, and the spectrum allocations from step 3).

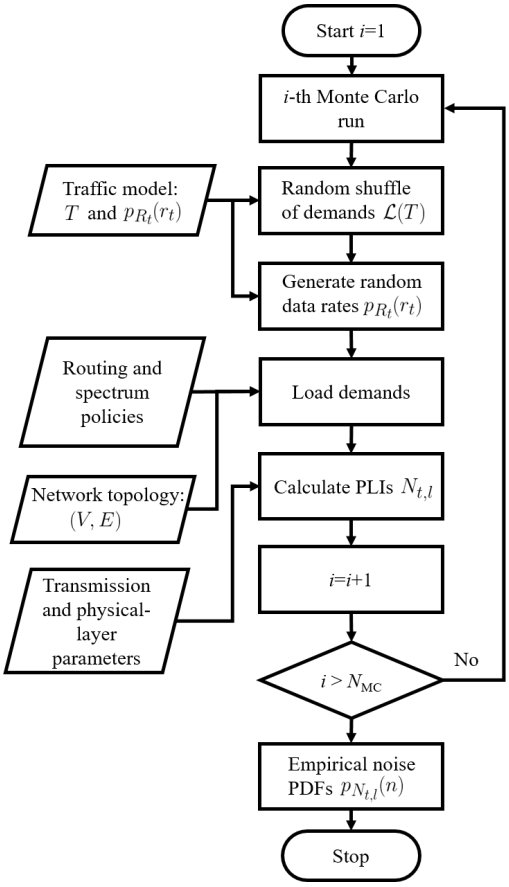

Figure 1: The modified SNAP that statistically characterizes PLI noise distributions.

Based on N_{MC} Monte Carlo repetitions, we can obtain an empirical PDF $p_{N_{t,l}}(n)$ that describes the random noise $N_{t,l}$ for the demand t on the link l, for all $t \in T$ and $l \in P_t$.

B. RS Allocation Heuristic

By using the empirical PLI noise distributions generated from the modified SNAP simulations, the RLP heuristic minimizes the BP with a fixed number F_{max} of RSs. This is decomposed into two subproblems: 1) finding a promising set of RS allocations with low BP and as few RSs as possible for each demand, and 2) selecting one RS allocation from the promising set of each demand such that the overall RS allocation achieves a low BP and the number of RSs is no larger than F_{max}.

We use $H_t(\mathbf{f})$ to denote the BP of demand $t \in T$ as a function of the RS allocation $\mathbf{f}$ in the network, where $\mathbf{f}$ is a vector of f_i for all $i \in V$, and f_i is a binary indicator that equals 1 if node i is an RS and 0 otherwise. Suppose $\mathbf{f}$ divides the route of t into a set of transparent segments $\texttt{Seg}(t, \mathbf{f})$. The evaluation of $H_t(\mathbf{f})$ for a given $\mathbf{f}$ is as follows:

1) Obtain $p_{N_t^s}(n)$, the PDF of the random accumulated PLI noise N_t^s at the end of the transparent segment $s \in \texttt{Seg}(t, \mathbf{f})$, based on the simulation data in the modified SNAP. Here we have

$$N_t^s = \sum_{l \in s} N_{t,l}, \tag{1}$$

and

$$p_{N_t^s}(n) = \circledast_{l \in s} p_{N_{t,l}}(n), \tag{2}$$

where the right-hand side of (2) is the convolution of all the $p_{N_{t,l}}(n)$ along s.

2) Calculate the BP H_t^s on the transparent segment s with

$$H_t^s = \int_{G/\text{SNR}_{\text{th}}}^{+\infty} p_{N_t^s}(n) dn. \tag{3}$$

3) Calculate $H_t(\mathbf{f})$ under the assumption that the BPs on disjoint transparent segments are independent by using

$$H_t(\mathbf{f}) = 1 - \Pi_{s \in \texttt{Seg}(t,\mathbf{f})}(1 - H_t^s), \tag{4}$$

or equivalently

$$-\ln(1 - H_t(\mathbf{f})) = -\sum_{s \in \texttt{Seg}(t,\mathbf{f})} \ln(1 - H_t^s). \tag{5}$$

To obtain the promising set of RS allocations that contains the optimal solution for the demand t, we first calculate H_t^s for all $s \in \texttt{Seg}(t)$, where $\texttt{Seg}(t)$ is the set of all possible transparent segments on the route of t. Then we construct a weighted complete graph $\bar{D}_t = (\bar{V}_t, \texttt{Seg}(t))$ with the set of nodes $\bar{V}_t = \{\texttt{src}(t), \texttt{dst}(t)\} \cup Q_t$, the set of links as $\texttt{Seg}(t)$, and the weight w_s associated with the link $s \in \texttt{Seg}(t)$ as

$$w_s = \begin{cases} -\ln(1 - H_t^s), & \text{if } H_t^s < 1, \\ +\infty, & \text{if } H_t^s = 1, \end{cases} \tag{6}$$

where Q_t is the ordered set of nodes on the route of t. In $\bar{D}_t$ the nodes on a path between $\texttt{src}(t)$ and $\texttt{dst}(t)$ is equivalent to an RS allocations on the route of t, and the total path weight corresponds to the BP of the RS allocation according to (5). We identify the promising set of RS allocations with $k-1$ RSs by an exhaustive search of the K-shortest weighted paths in $\bar{D}_t$ with k transparent segments. This search is summarized in Algorithm 1, where the following optimization is solved for different values of k.

$$\underset{u_s}{\text{minimize}} \quad \sum_{s \in \texttt{Seg}(t)} w_s u_s \tag{7a}$$

$$\text{subject to} \quad \sum_{\substack{s \in \texttt{Seg}(t) \\ \texttt{src}(s) = i}} u_s - \sum_{\substack{s \in \texttt{Seg}(t) \\ \texttt{dst}(s) = i}} u_s = \begin{cases} 1, & \text{if } i = \texttt{src}(t), \\ -1, & \text{if } i = \texttt{dst}(t), \\ 0, & \text{otherwise}, \end{cases} \quad \forall i \in \bar{V}, \tag{7b}$$

$$\sum_{s \in \texttt{Seg}(t)} u_s = k, \tag{7c}$$

$$\sum_{\substack{s \in \texttt{Seg}(t) \\ u_s^\kappa = 1}} u_s < 1, \quad \forall \kappa \in \{1, \ldots, |\mathcal{S}_{t,k}|\}. \tag{7d}$$

Here u_s for $s \in \texttt{Seg}(t)$ is a binary variable that equals 1 if the transparent segment s has its two endpoints as RSs, source, or destination of t and 0 otherwise. $\mathcal{S}_{t,k}$ is the set of solutions obtained at previous solvings of (7) with k transparent segments. u_s^κ is the value of u_s in the κ-th element of $\mathcal{S}_{t,k}$ for $\kappa \in \{1, \ldots, |\mathcal{S}_{t,k}|\}$. The objective (7a) calculates the BP of the demand t. Equation (7b) is the flow conservation constraint. Equation (7c) is a constraint on the number of transparent segments. Inequality (7d) searches for new solutions by excluding those already found. In other words, provided that (7c) is satisfied by u_s and u_s^κ for all $s \in \texttt{Seg}(t)$ and $\kappa \in \{1, \ldots, |\mathcal{S}_{t,k}|\}$, (7d) guarantees that $u_s \neq u_s^\kappa$ is held for at least one s and every κ such that the new solution is not identical to any previously found one.

Algorithm 1 Search of potential RS allocations for $t, t \in T$

Input:

- The weighted complete graph $\bar{D}_t = (\bar{V}, \texttt{Seg}(t))$ with link weights specified in (6)
- A constant K giving the number of RS solutions with the same number of transparent segments that will be searched

Let $\mathcal{S}_t$ denote the set of promising RS allocations
Initialize $\mathcal{S}_t = \varnothing$
for k in $\{1, \ldots, |Q_t| - 1\}$ **do**
    Let $\mathcal{S}_{t,k}$ denote the set of RS allocations with exactly k RSs
    Initialize $\mathcal{S}_{t,k} = \varnothing$
    for j in $\{1, \ldots, K\}$ **do**
        Solve (7) and convert its solution and objective value to an RS allocation $\mathbf{f}$ and BP $H_t(\mathbf{f})$, respectively
        $\mathcal{S}_{t,k} \leftarrow \mathcal{S}_{t,k} \cup \{\mathbf{f}\}$
    end for
    $\mathcal{S}_t \leftarrow \mathcal{S}_t \cup \mathcal{S}_{t,k}$
end for

Output: The set of all potential paths $\mathcal{S}_t$ and the corresponding NPBs $H_t(\mathbf{f}), \forall \mathbf{f} \in \mathcal{S}_t$

Based on the sets of promising RS allocations for all demands, we can select the overall RS allocation that satisfies the constraint on the number of RSs and achieves the minimum BP by solving the optimization problem

$$\underset{y_{t,\kappa}, z_i}{\text{minimize}} \quad \sum_{t \in T} \sum_{\kappa \in \mathcal{U}_t} y_{t,\kappa} H(\mathbf{f}^{t,\kappa}) \tag{8a}$$

$$\text{subject to} \quad \sum_{\kappa \in \mathcal{U}_t} y_{t,\kappa} = 1, \quad \forall t \in T, \tag{8b}$$

$$\sum_{t \in T} \sum_{\kappa \in \mathcal{U}_t} f_i^{t,\kappa} y_{t,\kappa} \leq \theta z_i, \quad \forall i \in V, \tag{8c}$$

$$\sum_{i \in V} z_i \leq F_{\max}. \tag{8d}$$

Here $\mathcal{U}_t = \{1, \ldots, |\mathcal{S}_t|\}$ is the set of indices for elements in $\mathcal{S}_t$, the binary variable $y_{t,\kappa}$ indicates if the precalculated solution $\mathbf{f}^{t,\kappa} \in \mathcal{S}_t$ is selected into the final RS allocation, the binary variable z_i indicates if the node $i \in V$ is chosen as an RS, $f_i^{t,\kappa}$ is the i-th element of $\mathbf{f}^{t,\kappa}$, θ is a large enough number, and $F_{\max}$ is the maximum number of RSs in the network. The objective (8a) calculates the overall BP in the network, (8b) implies that one RS allocation from $\mathcal{S}_t$ is chosen for each demand $t \in T$, (8c) calculates the RS allocation for each node,

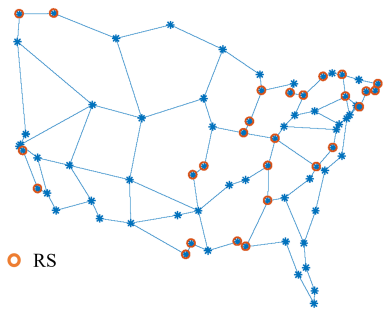

Figure 2: CONUS network topology. Circles represent an example RS allocation.

and (8d) is the constraint on the number of RSs.

The complexity of the proposed method is mainly attributed to the modified SNAP, whose required computational resources grow proportionally with the number of simulations N_{MC}. The RS allocation heuristic, however, has a comparatively low computational complexity due to the relatively simple formulations in (7) and (8), as measured by the number of variables involved.

IV. Numerical Results

In this section, we present simulation results for the proposed RS allocation heuristic. We first verify the accuracy of our BP estimation, next study the impact of data-rate-variable traffic demands on BP, and then compare it with two previous algorithms [6], [10] based on the TR model and static traffic prediction. The first benchmark is the greedy constrained-routing RLP (greedy-CRLP) [6] that minimizes the number of RSs subject to a certain routing constraint (in most cases, it is the shortest path constraint), a static traffic matrix, and a provided TR. The second benchmark is the routing and reach heuristic (RR) [10] that ranks the likelihood of being an RS for each node based on the network connectivity and TR model. This likelihood rank of nodes can also be obtained with the proposed algorithm by varying the value of $F_{\max}$ and recording the increment of $S(F_{\max})$. The BP and node ranking performances of the proposed algorithm are studied against the greedy-CRLP and RR, respectively, in the data-rate-variable scenario with the same TRs.

The continental US topology (CONUS) with 75 nodes and 99 bidirectional links shown in Fig. 2 is studied in the numerical simulations. We assume that there is one traffic demand between each node pair. The shortest distance routes and first-fit spectrum allocation scheme are used for all the traffic demands. Polarization-multiplexing quadrature phase shift keying with Nyquist spectral shaping is applied to all the traffic demands to obtain a spectral efficiency of 4 bits/s/Hz. A uniform and fixed PSD $G = 15$ W/THz is applied to all the traffic demands. The subcarrier bandwidth is $b_{\text{sub}} = 12.5$ GHz on all the fiber links. The demand data rate R_t is assumed to follow a normal distribution, i.e., $R_t \sim N(\mu, \sigma^2)$, for all the demands $t \in T$, with $\mu = 200$ Gbps and $\sigma = 20$ Gbps.

In the modified SNAP, $N_{\text{MC}} = 7 \times 10^4$ sets of random traffic are used to simulate the PLI noise distributions $p_{N_{t,l}}$. For performance verification, 3×10^4 sets of random traffic with shuffled spectrum orderings are used to simulate the BP. This gives an BP resolution of 3.3×10^{-5}, which corresponds to on average one noise blocking per demand in the whole BP simulation. Also observe that the accuracy of the PLI distributions output by the modified SNAP is dependable up to a certain confidence level. Therefore, the accuracy of the BP simulation as well as the PLI noise distributions can be improved by increasing the number of simulated traffic matrices in both parts, respectively.

Note that the benchmarks require the TR value as input, which is determined by the SNR threshold of the chosen transmission scheme and the fiber and amplifier parameters. To make a thorough comparison with the benchmarks in all possible cases, we vary the TR value from 1300 km to 5000 km by scaling the SNR threshold proportionally, which corresponds to different coding schemes and error-correction capacities. Moreover, the simulation results over different TR values can also help us to understand in what transmission scenarios the proposed algorithm is effective. Observe that in our proposed method, the TR values, or equivalently the SNR thresholds, are used in (3) to represent the susceptibility of traffic demands to PLIs, whereas the GN model is still used to calculate the actual PLIs.

BP estimation accuracy: The BPs predicted by (8) is compared with the simulation results in Fig. 3 for different TR values. The BPs are shown as functions of the number of RSs. The simulated and predicted BPs are close to each other, which means that the modified SNAP can empirically depict the PLI distributions well. The simulated curves have slightly higher BPs than the predicted ones because the results of the proposed algorithm is based on the empirical PLI distributions and, thus, suffers a slight BP performance degradation when generalized to new traffic matrices.

Impact of data-rate-variable traffic: Figure 4 illustrates the impact of variable data rate by simulating the BPs of demands with zero standard deviation. The RS allocations are based

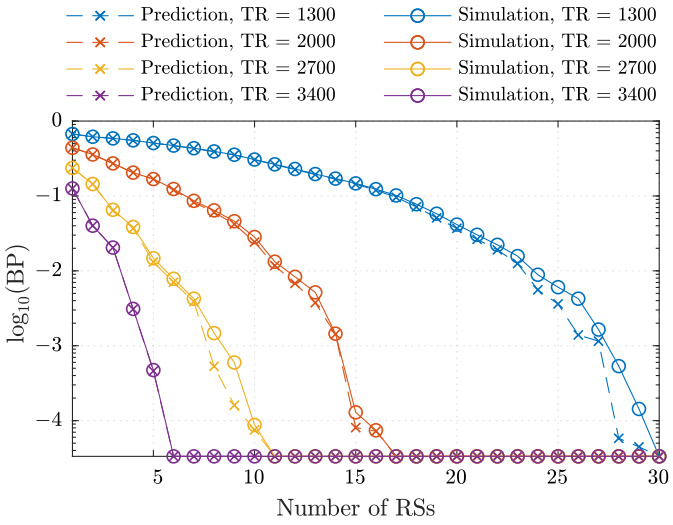

Figure 3: The BPs of the prediction and simulation with different TRs.

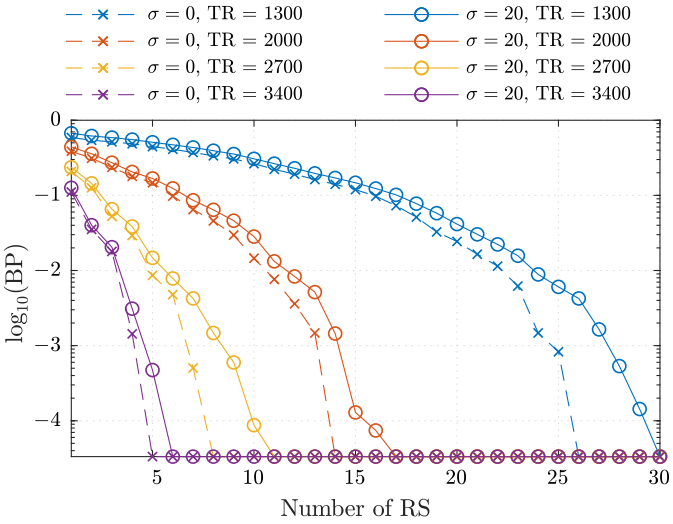

Figure 4: The simulated BPs for traffic demands with different standard deviations of data rates.

on the traffic with $\sigma = 20$ Gbps. The larger variance causes stronger PLIs for some of the demands and results in higher overall BPs. The zero variance traffic has less randomness in the PLI noise and, thus, has lower BPs. Therefore, it is necessary to consider the variable traffic in the RLP in nonlinear flexible-grid networks.

Comparison with the greedy-CRLP: In Fig. 5 the required numbers of RSs to achieve the same level of BPs at different TRs are compared for both the proposed algorithm and greedy-CRLP. At each TR, the greedy-CRLP computes one RS set and its corresponding BP, whereas the proposed algorithm can generate multiple RS sets, each for a different $F_{\max}$. To make a comparison between the two methods, we sweep $F_{\max}$ and choose the smallest one that achieves an BP no larger than that of the greedy-CRLP. As shown in Fig. 5, the proposed algorithm requires fewer RSs than the greedy-CRLP for most of the TRs. The average reduction in the number of RSs is around 10%.

Overprovision of the TR model: To study the impact of the PLI models in the RLP, we analyze the PLI PSD of the

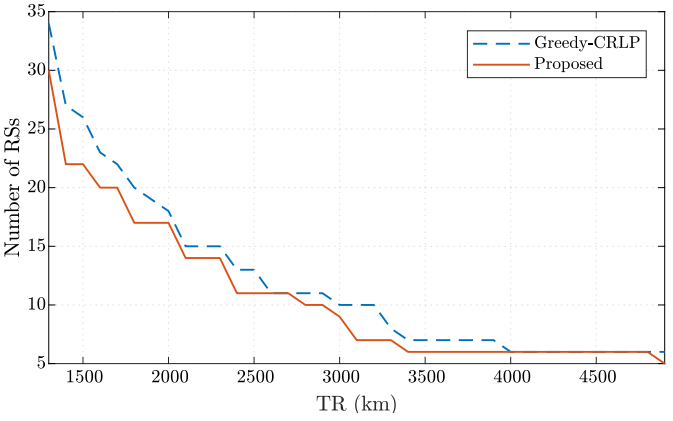

Figure 5: The number of RSs required by the proposed and greedy-CRLP algorithms to achieve similar BPs.

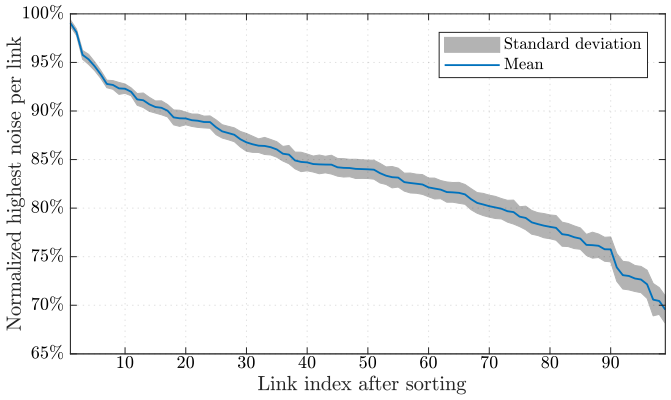

Figure 6: The highest PLI noise per link from the GN model normalized to the worst case from the TR model. The link indices are sorted in such a way that the means are in a descending order.

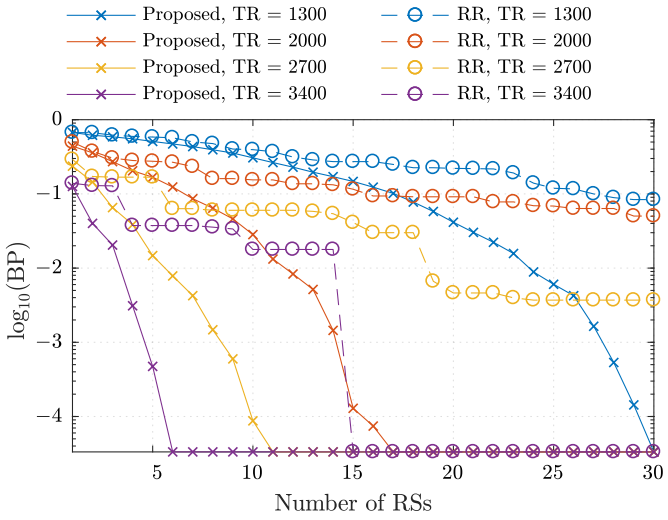

Figure 7: The BPs of the proposed and RR methods for different TRs and numbers of RSs.

demand with the highest impairments on each link calculated by the GN model, which is normalized to the worst case PLI noise estimated by the TR model. The means and standard deviations of the normalized noise are plotted in Fig. 6. We observe that the TR model tends to overestimate the PLIs with an average overestimation of 17%, which leads to an inefficient placement of RSs. This is because the TR model assumes that all the links are fully occupied, which is not the case in the network scenario due to the inevitable spectrum segmentation in the absence of wavelength converters.

Comparison with the RR: We compare the node ranking of being an RS calculated by the proposed and RR methods by visualizing their resulting BPs in Fig. 7. The BPs of different TRs are plotted as functions of the number of RSs for both methods. In the RR method, a node gets a higher rank if it is chosen as an RS by more traffic demands. As a result, two highly ranked nodes in the RR can be used to serve similar demands and are not necessary to be RSs at the same time. If we select both of them as RSs, the BP will not gain

much but the RS resources are wasted. This is the reason for the plateau areas in the RR curves in Fig. 7. In contrast, by optimizing the RS in combination instead of individually based on the empirical PLI distributions, the proposed algorithm achieves significantly lower BPs compared with the RR, with an average BP gain of two orders of magnitude.

V. Conclusion

The paper tackles the RLP in nonlinear flexible-grid networks with variable data rate requests. The GN model and modified SNAP framework are applied to statistically describe the PLI noise distribution of each demand–link pair in the network, based on which the set of RSs are determined. The proposed method also predicts the BP performance of its solution. The efficiency of the allocated RS set is improved compared with previous studies by estimating the PLI more accurately and taking into account the realistic traffic conditions in the network.

VI. Acknowledgment

Parts of this paper have been presented at the Optical Fiber Communication Conference (OFC), San Diego, CA, March 2018. This research is supported in part by the NSF Grant CCF-1422871, the Swedish Research Council Grant 2012-5280, and the Ericsson Research Foundation.

References

[1] O. Gerstel, M. Jinno, A. Lord, and S. Yoo, "Elastic optical networking: A new dawn for the optical layer?" *IEEE Communications Magazine*, vol. 50, no. 2, pp. 12–20, 2012.

[2] M. Jinno, H. Takara, B. Kozicki, Y. Tsukishima, Y. Sone, and S. Matsuoka, "Spectrum-efficient and scalable elastic optical path network: Architecture, benefits, and enabling technologies," *IEEE Communications Magazine*, vol. 47, no. 11, pp. 66–73, 2009.

[3] L. Beygi, E. Agrell, J. M. Kahn, and M. Karlsson, "Rate-adaptive coded modulation for fiber-optic communications," *IEEE Journal of Lightwave Technology*, vol. 32, no. 2, pp. 333–343, 2014.

[4] N. Sambo, G. Meloni, F. Cugini, A. D'Errico, L. Potì, P. Iovanna, and P. Castoldi, "Routing code and spectrum assignment (RCSA) in elastic optical networks," *IEEE Journal of Lightwave Technology*, vol. 33, no. 24, pp. 5114–5121, 2015.

[5] J. Zhao, L. Yan, H. Wymeersch, and E. Agrell, "Code rate optimization in elastic optical networks," in *Proc. European Conference on Optical Communication (ECOC)*, Valencia, Spain, Sept. 2015, p. We.3.5.1.

[6] B. G. Bathula, R. K. Sinha, A. L. Chiu, M. D. Feuer, G. Li, S. L. Woodward, W. Zhang, R. Doverspike, P. Magill, and K. Bergman, "Constraint routing and regenerator site concentration in ROADM networks," *Journal of Optical Communications and Networking*, vol. 5, no. 11, pp. 1202–1214, 2013.

[7] B. G. Bathula, A. L. Chiu, R. K. Sinha, and S. L. Woodward, "Routing and regenerator planning in a carrier's core ROADM network," in *Proc. Optical Fiber Communication Conference (OFC)*, Los Angeles, CA, Mar. 2017, pp. Th4F–4.

[8] F. Kuipers, A. Beshir, A. Orda, and P. Van Mieghem, "Impairment-aware path selection and regenerator placement in translucent optical networks," in *Proc. International Conference on Network Protocols (ICNP)*. Kyoto, Japan: IEEE, 2010, pp. 11–20.

[9] S. Varma and J. P. Jue, "Regenerator placement and waveband routing in optical networks with impairment constraints," in *Proc. International Conference on Communications (ICC)*. Kyoto, Japan: IEEE, 2011, pp. ONSP–1.

[10] J. Pedro, "Predeployment of regenerators for fast service provisioning in DWDM transport networks," *Journal of Optical Communications and Networking*, vol. 7, no. 2, pp. A190–A199, 2015.

[11] S. Varma and J. P. Jue, "Regenerator site selection in mixed line rate waveband optical networks," *Journal of Optical Communications and Networking*, vol. 5, no. 3, pp. 198–209, 2013.

[12] W. Xie, J. P. Jue, X. Wang, Q. Zhang, Q. She, P. Palacharla, and M. Sekiya, "Regenerator site selection for mixed line rate optical networks," *Journal of Optical Communications and Networking*, vol. 6, no. 3, pp. 291–302, 2014.

[13] X. Wang, M. Brandt-Pearce, and S. Subramaniam, "Impact of wavelength and modulation conversion on transluscent elastic optical networks using MILP," *Journal of Optical Communications and Networking*, vol. 7, no. 7, pp. 644–655, 2015.

[14] E. Agrell, M. Karlsson, A. Chraplyvy, D. J. Richardson, P. M. Krummrich, P. Winzer, K. Roberts, J. K. Fischer, S. J. Savory, B. J. Eggleton *et al.*, "Roadmap of optical communications," *Journal of Optics*, vol. 18, no. 6, p. 063002, 2016.

[15] A. Leiva, C. M. Machuca, A. Beghelli, and R. Olivares, "Migration cost analysis for upgrading WDM networks," *IEEE Communications Magazine*, vol. 51, no. 11, pp. 87–93, 2013.

[16] A. Zapata-Beghelli and P. Bayvel, "Dynamic versus static wavelength-routed optical networks," *Journal of Lightwave Technology*, vol. 26, no. 20, pp. 3403–3415, 2008.

[17] P. Poggiolini, G. Bosco, A. Carena, V. Curri, Y. Jiang, and F. Forghieri, "The GN-model of fiber non-linear propagation and its applications," *IEEE Journal of Lightwave Technology*, vol. 32, no. 4, pp. 694–721, 2014.

[18] P. Johannisson and E. Agrell, "Modeling of nonlinear signal distortion in fiber-optic networks," *IEEE Journal of Lightwave Technology*, vol. 32, no. 23, pp. 3942–3950, 2014.

[19] L. Yan, E. Agrell, H. Wymeersch, and M. Brandt-Pearce, "Resource allocation for flexible-grid optical networks with nonlinear channel model," *Journal of Optical Communications and Networking*, vol. 7, no. 11, pp. B101–B108, 2015.

[20] M. Cantono, R. Gaudino, and V. Curri, "Potentialities and criticalities of flexible-rate transponders in DWDM networks: A statistical approach," *Journal of Optical Communications and Networking*, vol. 8, no. 7, pp. A76–A85, 2016.

[21] R. Schmogrow, M. Winter, M. Meyer, D. Hillerkuss, S. Wolf, B. Baeuerle, A. Ludwig, B. Nebendahl, S. Ben-Ezra, J. Meyer *et al.*, "Real-time Nyquist pulse generation beyond 100 Gbit/s and its relation to OFDM," *Optics Express*, vol. 20, no. 1, pp. 317–337, 2012.

[22] F. Cugini, F. Paolucci, G. Meloni, G. Berrettini, M. Secondini, F. Fresi, N. Sambo, L. Poti, and P. Castoldi, "Push-pull defragmentation without traffic disruption in flexible grid optical networks," *Journal of Lightwave Technology*, vol. 31, no. 1, pp. 125–133, 2013.

[23] A. Asensio, M. Klinkowski, M. Ruiz, V. López, A. Castro, L. Velasco, and J. Comellas, "Impact of aggregation level on the performance of dynamic lightpath adaptation under time-varying traffic," in *Proc. IEEE International Conference of Optical Network Design and Modeling (ONDM)*, Brest, France, Apr. 2013, pp. 184–189.

[24] L. Velasco, A. P. Vela, F. Morales, and M. Ruiz, "Designing, operating, and reoptimizing elastic optical networks," *Journal of Lightwave Technology*, vol. 35, no. 3, pp. 513–526, 2017.